

Pasquale Cavaliere

Fatigue and Fracture of Nanostructured Materials

 Springer

Fatigue and Fracture of Nanostructured Materials

Pasquale Cavaliere

Fatigue and Fracture of Nanostructured Materials

 Springer

Pasquale Cavaliere
Department of Innovation Engineering
University of Salento
Lecce, Italy

ISBN 978-3-030-58087-2 ISBN 978-3-030-58088-9 (eBook)
<https://doi.org/10.1007/978-3-030-58088-9>

© Springer Nature Switzerland AG 2021

This work is subject to copyright. All rights are reserved by the Publisher, whether the whole or part of the material is concerned, specifically the rights of translation, reprinting, reuse of illustrations, recitation, broadcasting, reproduction on microfilms or in any other physical way, and transmission or information storage and retrieval, electronic adaptation, computer software, or by similar or dissimilar methodology now known or hereafter developed.

The use of general descriptive names, registered names, trademarks, service marks, etc. in this publication does not imply, even in the absence of a specific statement, that such names are exempt from the relevant protective laws and regulations and therefore free for general use.

The publisher, the authors, and the editors are safe to assume that the advice and information in this book are believed to be true and accurate at the date of publication. Neither the publisher nor the authors or the editors give a warranty, expressed or implied, with respect to the material contained herein or for any errors or omissions that may have been made. The publisher remains neutral with regard to jurisdictional claims in published maps and institutional affiliations.

This Springer imprint is published by the registered company Springer Nature Switzerland AG
The registered company address is: Gewerbestrasse 11, 6330 Cham, Switzerland

Preface

Nanostructured materials represent a possible alternative for a broader range of applications, outperforming many of today's engineering materials. As new nanomaterials are rapidly developing and many applications exist, mainly within fields such as medicine, communication, consumer goods, and engineering, it is necessary to identify what special properties this fairly new material group can offer. All engineering materials based on nanotechnology, involving the understanding of physical properties and how they change with material dimensions, are to be considered alternatives in existing products.

Metals with a grain size in the range of 100–1000 nm are classified as ultrafine grain; grain sizes less than 100 nm are considered to be in the nanocrystalline domain. The altered response of such properties is a direct consequence of the nanoscale microstructural arrangements of the atoms themselves. Regarding engineering design, these metals pose significant promise as next-generation structural materials due to reported increases in ultimate strength, resistance to fatigue, and wear resistance.

The abnormally high volume fractions of noncrystalline material exaggerate the importance of the grain boundaries, ultimately leading to a shift in the physical plasticity mechanisms which take place during deformation. At the smallest grain sizes traditional intragranular dislocation-based mechanisms begin to shut off which leads to the dominance of grain boundary-mediated mechanisms.

The main routes employed to produce UFG and NC materials are presented by underlying the pros and cons of the application of each production from mechanical alloying and severe plastic deformation to electrodeposition, sputtering, and surface modification. All those mechanisms, active at the nanoscale, governing the crack initiation and growth behavior as well as the crack-grain-microstructural features, are theoretically described. The strength-ductility effect on the fatigue life of nanocrystalline materials with particular attention to cyclic plastic strain is discussed. The effect of grain boundary strengthening through alloying with the related consequences on the fatigue life and fatigue mechanisms acting during cyclic deformation is underlined. The different behaviors due to the various mechanisms acting during

creep in nanocrystalline metals and alloys have been described. The effect of nanostructuring on the creep and superplastic behavior of metals and alloys is also shown. The different mechanical behavior of thin films due to the reduced thickness and the confined deformation mechanisms is described as well. How mechanical properties of thin films differ from those of bulk materials is underlined. The wear behavior related to the effect of grain refinement and the consequent grain-mediated deformation mechanisms is shown. The contact fatigue and fretting mechanisms acting in nanostructured metals and alloys are also described. The cycle sliding-activating fatigue mechanisms in nanostructured metals and alloys are shown too.

My special thanks to the professionalism of the editorial office manager and assistants. I would like to dedicate this book to my son Paolo.

Lecce, Italy

Pasquale Cavaliere

Contents

1	Nanostructuring of Metals, Alloys, and Composites	1
1.1	Introduction	1
1.2	Nanostructured Material Synthesis	18
1.2.1	Mechanical Alloying	20
1.2.2	Severe Plastic Deformation	26
1.2.3	Electrodeposition	48
1.3	Conclusions	52
	References	53
2	Cyclic Deformation of Metal Alloys and Composites	59
2.1	Introduction	59
2.2	Elastoplastic Behavior in Nanostructured Metals and Alloys	61
2.2.1	Dislocations and Plasticity	61
2.2.2	Cyclic Behavior	77
2.3	Nanoindentation	90
2.3.1	Cyclic Nanoindentation	95
2.4	Conclusions	98
	References	100
3	Crack Initiation and Growth in Metal Alloys and Composites	105
3.1	Introduction	105
3.1.1	Dislocation Sources	106
3.1.2	GB Mechanisms	109
3.1.3	Grain Growth	110
3.1.4	Dislocation Absorption	111
3.1.5	Strain Rate Sensitivity	111
3.2	Grain Deformation at the Crack Tip	119
3.3	Mechanisms of Cracking in NC Materials	121
3.3.1	Crack Behavior in NC Materials	121

3.4	Crack Initiation and Growth in Nanostructured Materials	128
3.4.1	Fatigue Cracks in NC Materials	128
3.4.2	Crack Propagation	131
3.4.3	Nanotwinning	136
3.5	Conclusions	151
	References	152
4	Fatigue and Crack Behavior of Nanostructured Metal Alloys and Composites	155
4.1	Introduction	155
4.1.1	Effect of Strain Rate	158
4.1.2	Dislocation-GB Interaction	164
4.2	Fatigue Life of NC Materials	175
4.2.1	Fatigue Endurance in NC Metals and Alloys	175
4.3	Crack Initiation and Growth in Nanocrystalline Materials	183
4.3.1	Fracture Behavior in NC Materials	184
4.3.2	Cyclic Behavior of Graded Materials	193
4.3.3	Cyclic Indentation of Graded NC Materials	204
4.4	Conclusions	216
	References	217
5	Fatigue and Crack Behavior of Bulk Nanostructured Metal Alloys and Composites	221
5.1	Introduction	221
5.1.1	Anisotropy in SPDed Materials	227
5.2	Fatigue Life of UFG Materials	228
5.2.1	Deformation Mechanisms in UFGed Materials	229
5.2.2	Fatigue Life of UFGed Materials	231
5.3	Damage Tolerance of UFG Materials	242
5.3.1	Crack Initiation and Growth in UFGed Materials	242
5.3.2	Microstructural Behavior of Deformed UFGed Materials	251
5.4	Conclusions	255
	References	257
6	Creep in Nanostructured Materials	263
6.1	Introduction	263
6.1.1	Creep Mechanisms	263
6.1.2	Creep Characterization of NC Materials	268
6.1.3	Microstructural Features	272
6.2	Creep in UFG Materials	274
6.2.1	Effect of SPD	274
6.2.2	Creep Rate in UFGed Materials	275
6.3	Creep in NC Materials	278
6.3.1	Creep Mechanisms in NC Materials	279
6.3.2	Strain Rate Effect	280

6.4	Creep in Thin Films	285
6.4.1	Size Effect	286
6.5	Conclusions	291
	References	292
7	Superplasticity in Nanostructured Materials	297
7.1	Introduction	297
7.1.1	Grain Boundary Sliding	298
7.1.2	Diffusion	298
7.1.3	Constitutive Relationships	302
7.2	Superplasticity in SPD Materials	303
7.2.1	Grain Development Behavior	305
7.2.2	Uniform Elongation	307
7.2.3	Mechanisms in UFGed Materials	310
7.3	Superplasticity in Nanocrystalline Materials	313
7.3.1	Grain Size Effect on Superplastic Behavior	314
7.3.2	Dislocation Behavior	315
7.4	Conclusions	328
	References	330
8	Mechanical Properties of Thin Films and Coatings	333
8.1	Introduction	333
8.1.1	Microstructural Evolution in Thin Films	335
8.1.2	Grain Evolution	337
8.2	Mechanical Properties of Thin Films	338
8.2.1	Thin-Film Strength	338
8.3	Fatigue of Nanostructured Thin Films	344
8.3.1	Fatigue Mechanisms in Thin Films	344
8.3.2	Size Effect	346
8.3.3	Fracture Behavior	349
8.3.4	Grain Boundary Structure	356
8.4	Conclusions	362
	References	363
9	Contact Fatigue and Crack Behavior of Nanostructured Metal Alloys and Composites	367
9.1	Introduction	367
9.2	Wear Mechanisms in Nanostructured Materials	368
9.2.1	Wear Characterization	369
9.2.2	Scratch Behavior	374
9.3	Fretting in Nanostructured Materials	376
9.3.1	Fretting Mechanisms	378
9.3.2	Size Effect	382
9.4	Conclusions	384
	References	384

10 Effect of Environment on Microstructure and Mechanical Properties of Nanostructured Metal Alloys and Composites 387

10.1 Introduction 387

10.2 Corrosion of Nanostructured Materials 389

10.3 SCC in Nanostructured Materials 401

10.4 Conclusions 408

References 409

Index 411

Abbreviations

AA	Aluminum alloy
AD	Axial direction
AGG	Abnormal grain growth
AIF	Amorphous intergranular film
ALD	Atomic layer deposition
ALG	Abnormally large grain
AM	AMorphous
ARB	Accumulative roll-bonding
C/T	Compression/tension
CCC	Cylinder-covered compression
CF	Corrosion fatigue
CGB	Clean grain boundary
CGBS	Cooperative grain boundary sliding
CGP	Constrained groove pressing
CIP	Cold isostatic pressure
CO	Coble
CR	Cold rolling
CRSS	Critical resolved shear stress
CSL	Coincidence site lattice
CSS	Cyclic stress strain
CTB	Coherent twin boundaries
CVD	Chemical vapor deposition
DLC	Diamond-like carbon
DSC	Displacement shift complete
DSI	Depth-sensing indentation
DUFG	Deformed ultrafine grain
EAC	Environmentally assisted cracking
ECAP	Equal-channel angular pressing
EIS	Electrochemical impedance spectroscopy
F	Ferrite

FCB	Fatigue crack behavior
FCG	Fatigue crack growth
FEM	Finite element modeling
FGM	Functionally graded materials
FSP	Friction stir processing
GA	Grain agglomerates
GB	Grain boundary
GBAZ	Grain boundary-affected zone
GBCD	Grain boundary character distribution
GBD	Grain boundary dislocation
GBP	Grain boundary process
GBS	Grain boundary sliding
GNB	Geometrically necessary boundary
GNC	Gradient nanocrystalline
GND	Geometrically necessary dislocations
H	Hardness
HAGB	High-angle grain boundary
HCF	High-cycle fatigue
HE	Hydrogen embrittlement
HEA	High-entropy alloy
HESP	High-energy shot peening
HIP	Hot isostatic pressure
HNM	Heterogeneous nanostructured materials
H-P	Hall-Petch
HPT	High-pressure torsion
HSR	High strain rate
IDB	Incidental dislocation boundary
IGSCC	Intergranular stress corrosion cracking
IHPE	Inverse Hall-Petch effect
II	Ion implantation
ISE	Indentation size effect
ITB	Incoherent twin boundary
LAGB	Low-angle grain boundary
LBQ	Laser beam quenching
LCF	Low-cycle fatigue
LEDS	Low-energy dislocation structures
LP	Leading partial
LSNT	Large spacing nanotwinned
LSP	Laser shock peening
M	Martensite
MC	Microcrystalline
MD	Molecular dynamic
MDS	Molecular dynamic simulation
MEMS	Microelectromechanical systems

nc	Nanocrystalline
NEMS	Nanoelectromechanical systems
NH	Nabarro–Herring
NRD	Nanoscale rotational deformation
NS	Nanostructured
NT	Nanotwinned
OGBC	Ordered grain boundary complexion
PD	Partial dislocations
PGM	Plastically graded material
PIII	Plasma immersion ion implantation
P-N	Peierls–Nabarro
PN	Plasma nitriding
PSB	Persistent slip band
PZ	Plastic zone
RCS	Repetitive corrugation and straightening
RD	Radial direction
RHAGB	Random high-angle grain boundary
ROM	Rule of mixture
RPZ	Reversible plastic zone
S ² PD	Surface severe plastic deformation
SB	Slip bands
SCC	Stress corrosion cracking
SF	Stacking fault
SFE	Stacking fault energy
SFSP	Submerged friction stir processing
SIF	Stress intensity factor
SMAT	Surface mechanical attrition treatment
SMC	Submicrocrystalline
SMGT	Surface mechanical grinding treatment
SNH	Surface nano-crystallization and hardening
SP	Shot peening
SPD	Severe plastic deformation
SPS	Spark plasma sintering
SRS	Strain rate sensitivity
SS	Stainless steel
SSNT	Small spacing nanotwinned
SSP	Severe shot peening
STZ	Shear transformation zone
TB	Twin boundary
TD	Tangential directions
TJ	Triple junction
TL	Triple line
TP	Twin plane
TTS	Tribologically transformed structure

UDUFG	Undeformed ultrafine grain
UHP	Ultrahigh pressures
UNSM	Ultrasonic nanocrystal surface modification
UP	Ultrasonic peening
USP	Ultrasonic shot peening
USRP	Ultrasonic surface rolling processing
WIF	Wear induced by fretting

Chapter 1

Nanostructuring of Metals, Alloys, and Composites



1.1 Introduction

Nanostructured materials are the most potential and exciting candidates in many fields for revolutionizing traditional material designs. Nanostructured metals and alloys are a class of materials exhibiting novel characteristics across a wide range of properties including increased hardness, superplasticity, and electrical conductivity (Schaefer 2010). Here, the difference between ultrafine and nanocrystalline metals needs a special mention. Conventionally, metals with a grain size in the range of 100–1000 nm are classified as ultrafine grain; grain sizes less than 100 nm are considered to be in the nanocrystalline domain (Gleiter 1989, 1993).

The altered response of such properties is a direct consequence of the nanoscale microstructural arrangements of the atoms themselves (Murr 2015). Regarding engineering design, these metals pose significant promise as next-generation structural materials due to reported increases in ultimate strength, resistance to fatigue, and wear resistance (Mittemeijer 2010).

Nanostructured materials represent a possible alternative for a broader range of applications, outperforming many of today's engineering materials. As new nanomaterials are rapidly developing and many applications exist, mainly within fields such as medicine, communication, consumer goods, and engineering, it is necessary to identify what special properties this fairly new material group can offer. All engineering materials based on nanotechnology, involving the understanding of physical properties and how they change with material dimensions, are to be considered alternatives in existing products.

Through following the Hall-Petch equation

$$\sigma_y = \sigma_0 + \frac{k_y}{\sqrt{D}}$$

where σ_y is the yield strength, σ_0 is a material constant (i.e., 25 for Cu, 70 for Fe, and 80 for Ti), k_y represents the resistance of grain boundaries to dislocation mobility (transmission through grain boundaries) giving the quantification of the grain boundary strengthening (i.e., 0.11 for Cu, 0.74 for Fe, and 0.4 for Ti), and D is the mean grain size. A high density of grain boundaries limits the length of dislocation pileups and, due to restricted dislocation motion, extraordinarily high yield stress values can be observed (Gutkin and Ovid'ko 2004). However, the extraordinary mechanical properties of NC metals are limited by mechanisms related to the competing length scales (Anderson et al. 2014; Mohamed 2016).

The Hall-Petch relationship essentially describes grain boundary strengthening, a process by which grain boundaries, or regions between crystallites of different lattice orientation, act as physical barriers for continued dislocation movement within the material (Armstrong 2014). For more traditional, coarse-grained materials consisting of average grain sizes ranging from 100 nm upwards of several microns, gliding dislocations act as the main carriers of plasticity. For this reason, as grain size is decreased, significant strengthening can be expected (Brandl 2019). The core of this idea is that grain boundaries hinder dislocations, which accumulate and cause stress concentrations (Suryanarayana and Koch 2000). This resistance is thought to be proportional to the misalignment between the meeting slip systems and the magnitude of the burger's vector of the residual grain boundary dislocation that is created by transmission. The reliance on a planar dislocation pileup arrangement has led to criticism of this theory. In fact, it was revealed that the length of these pileups has not been correlated with grain size, nor are they likely to form in materials where cross-slip to other planes is relatively easy. Instead, a different explanation was proposed in which grain boundaries serve as nucleation sites for dislocations. The idea is that a greater grain boundary area will provide more dislocation sources and lead to a higher dislocation content at a given strain. Strength is known to depend on the square root of dislocation density. Another alternate explanation of the Hall-Petch effect has been offered by proposing that strain gradients imposed by compatibility requirements between grains increase the dislocation density. These strain gradients become larger as grain size decreases, and so does the number of geometrically necessary dislocation needed to support them.

A strong effort has been devoted to metal and alloy nanostructuring in order to reach the material's theoretical maximum strength ($G/10$). The pioneering view of Gleiter (1989) pushed the research on nanostructured metals in the recent decades. In the paper, nanocrystalline materials are defined as single- or multiphase polycrystals with nanoscale grain size (1–250 nm). As upper limit, “ultrafine grain” is used to indicate grain size in the range of 250–1000 nm. First of all, the properties of these materials are related to the increase of the grain boundary volume fraction as the mean grain size decreases. The abnormally high volume fractions of noncrystalline material exaggerate the importance of the grain boundaries, ultimately leading to a shift in the physical plasticity mechanisms which take place during deformation (Meyers et al. 2006a). At the smallest grain sizes traditional intragranular dislocation-based mechanisms begin to shut off which leads to the dominance of grain boundary-mediated mechanisms.

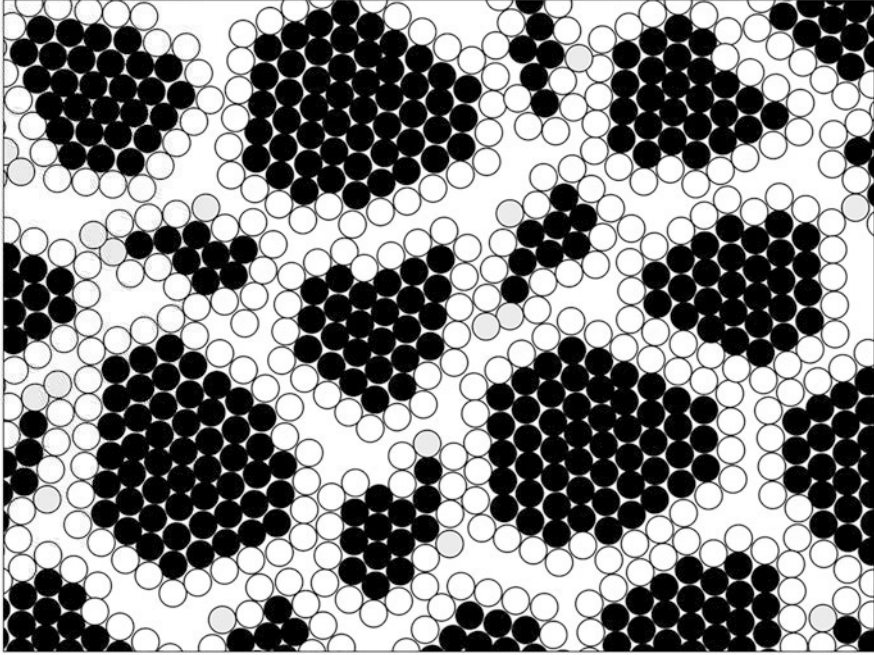


Fig. 1.1 2-D model of nanostructured materials

The altered response of NC material properties is a direct consequence of the nanoscale microstructural arrangements of the atoms themselves. The atoms in the crystal interior are closely packed in an ordered configuration; those in the grain boundaries are in a more chaotic high-energy configuration with a different spacing (Fig. 1.1).

As the grain size decreases, the nanocrystalline material interfaces contain higher atom fractions. For grain size in the order of magnitude of 5 nm the fraction is in the order of 50%; for 10 nm, the grain boundary volume fraction is around 30%; for ultrafine-grained materials it is around 2% while for microcrystalline metals and alloys it is orders of magnitude lower (Fig. 1.2).

Unfortunately, due to the high volume fractions of grain boundaries, the driving force for nanocrystalline grain growth is amplified (Andrievski and Khatchoyan 2016). Therefore, minimizing grain growth and maintaining their beneficial properties prove extremely challenging.

In nanocrystalline materials, the intercrystalline volume fraction is found to comprise as much as 50% of the total crystal volume. These solids are assumed to have a different kind of atomic structure: a crystalline structure with long-range order for all the atoms far from the grain boundaries and a disordered structure with some short-range order at the interfacial region. Hence, the mechanical properties of these nanocrystalline materials are expected to be different as compared to their equal polycrystalline material. There are two main strategies that have garnered the most

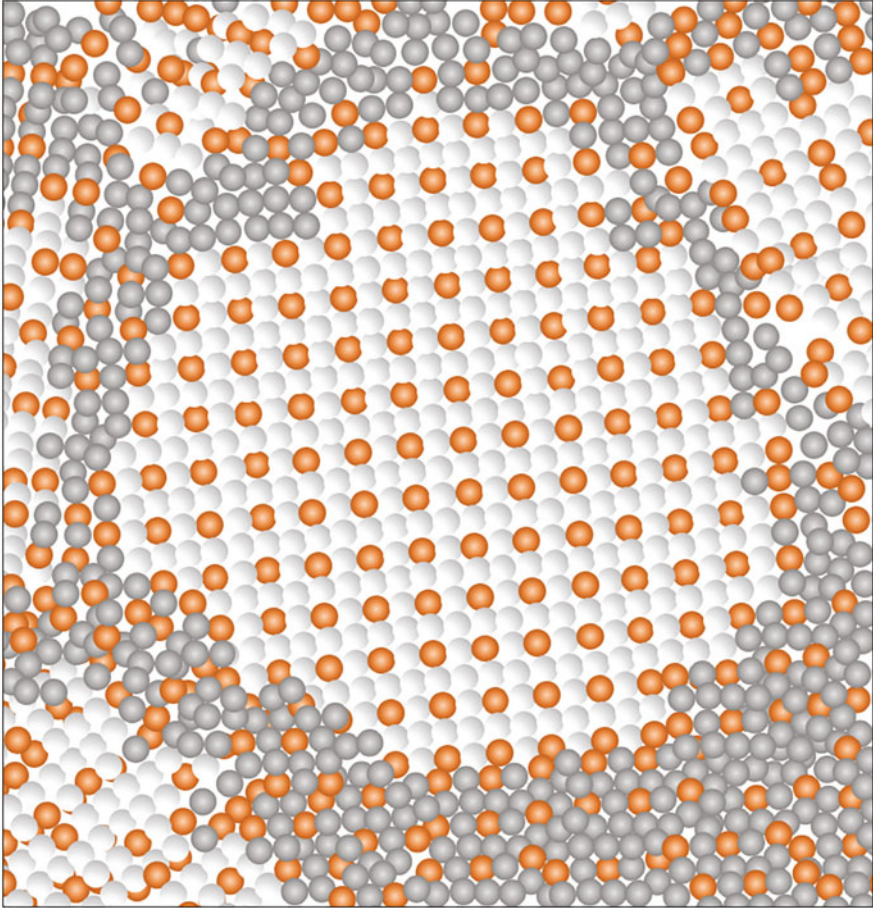


Fig. 1.2 MD model of nanocrystalline Ni-Fe with 5 nm grain size

attention. The first strategy utilizes kinetic mechanisms that decrease grain boundary mobility, such as solute drag, reduced diffusivity, particle drag, and chemical ordering. The second strategy utilizes solute segregation to reduce the grain boundary energy and consequently the driving force (Razumov 2014).

The grain boundary energy is given by the following equation:

$$\gamma = \gamma_0 - \Gamma(\Delta H^{\text{seg}} + RT \ln X)$$

where γ is the grain boundary energy, γ_0 is the original grain boundary energy of the pure metal, Γ is the grain boundary solute excess, ΔH_{seg} is the enthalpy of segregation, R is the Boltzmann constant, T is the temperature, and X is the global dopant composition. The equation ultimately means that segregation of dopant to grain

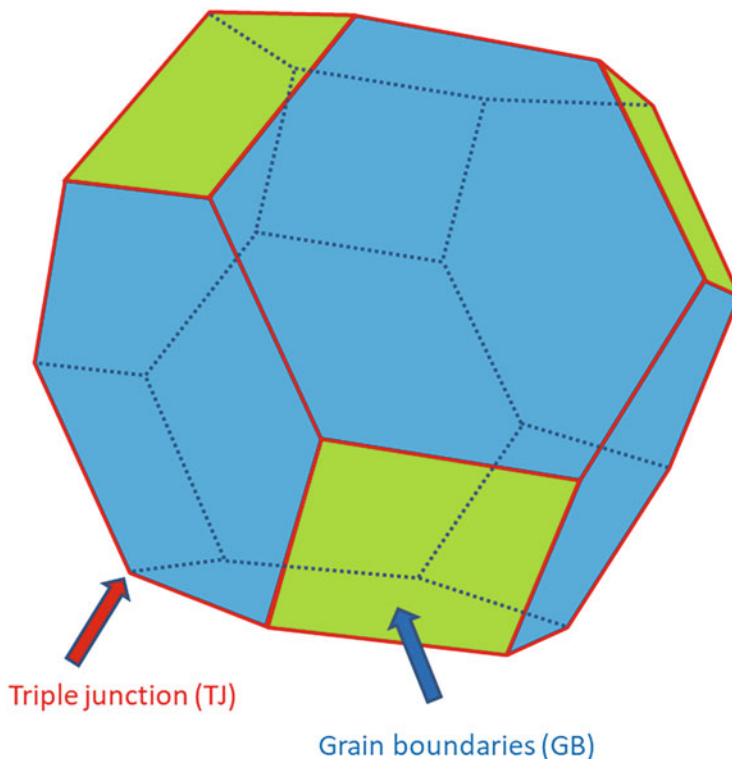


Fig. 1.3 Ideal tetrakaidecahedron grains with a grain boundary thickness of 1 nm

boundaries can lower the grain boundary energy and consequently change its behavior.

By analyzing this aspect through the employment of an ideal tetrakaidecahedron grain structure with a grain boundary thickness of 1 nm (Fig. 1.3), it is possible to plot the relationship between the grain size and the volume fraction.

So, both the volume fraction and the triple junctions increase as the mean grain size decreases (Fig. 1.4).

The dotted lines show the evolution of grain boundary thickness and its effect as a function of grain size (range 1–0.1 nm).

Experimental evidences show that GB size is around 0.5 nm for NC materials with FCC crystal structure and 1 nm for NC BCC crystal structure. From Fig. 1.5 it can be observed that for a grain size of 5 nm approximately 40% of the atoms lie in the grain boundary (Siegel and Thomas 1992; Spearot and McDowell 2009).

The volume fraction as a function of grain size distribution was measured for many Ni and Ni-Fe electrodeposited nanostructured materials (Fig. 1.6).

So, the overall behavior of nanocrystalline materials is dependent on not only the grain size but also the nature of grain boundary structures. Generally, these interfaces are responsible for the strength behavior of metals and alloys. The atom orientation

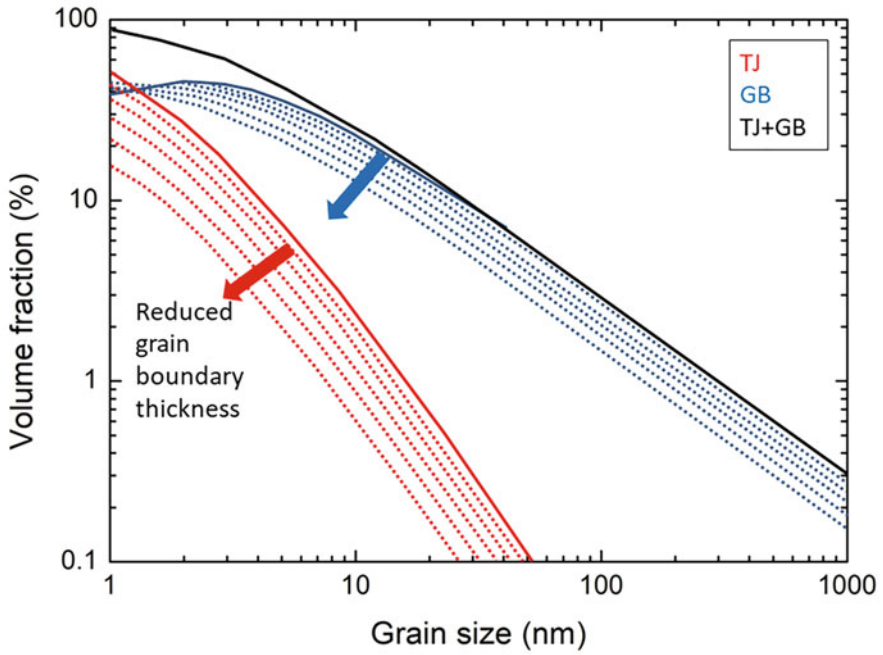


Fig. 1.4 Volume fraction and triple junctions as a function of the grain size

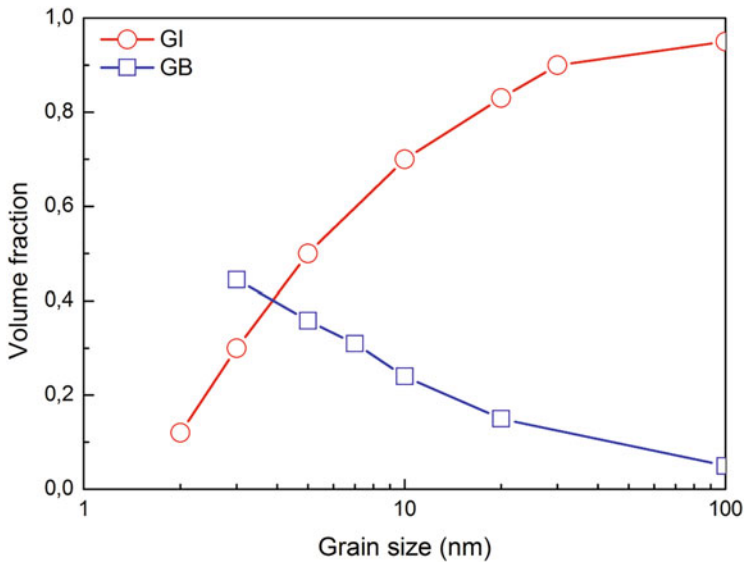


Fig. 1.5 Grain boundary vs. grain interior volume fraction

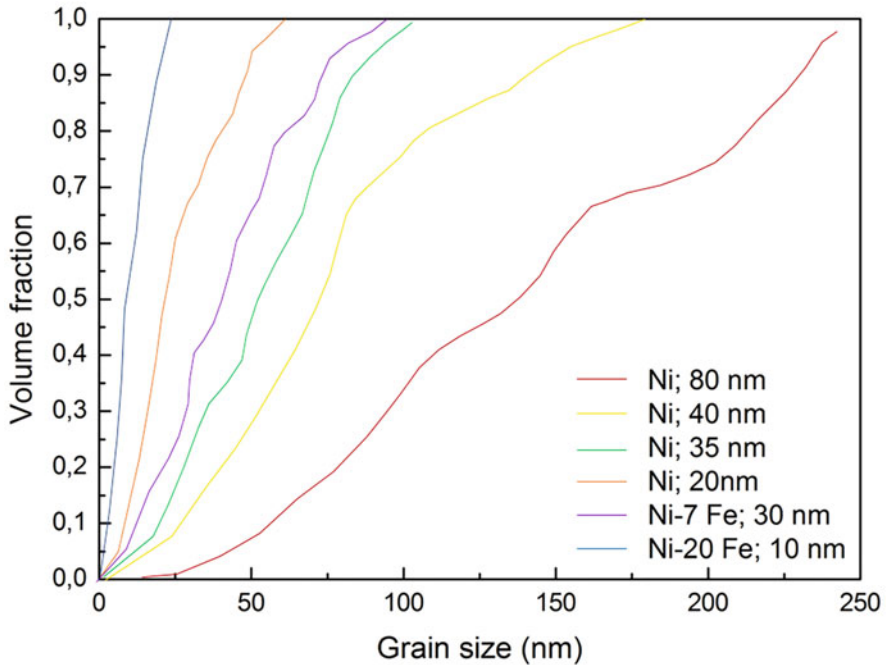


Fig. 1.6 Volume fraction vs. grain size distribution for different Ni and Ni-Fe

in adjacent grain is different; in addition, the atoms in the grain boundaries are in a disordered state. These factors lead to a difficulty for a dislocation to continuously slip in all the material volume because it must overcome the grain boundaries with a change in the slip direction (Fig. 1.7).

This hinders the material plasticity with a direct effect on the yield strength increase of the material (Sun 2014). The stress applied to the crystal (σ) generates a shear stress (τ_a); the crystal opposes a resistance (τ_0) to the generated shear stress (Fig. 1.8).

So, the effective stress (τ_{eff}) for the dislocation sliding is

$$\tau_{\text{eff}} = \tau_a - \tau_0$$

This is the model describing the situation in the grain interior. By approaching the grain boundary, the dislocation must have sufficient energy to overcome the grain boundary; otherwise it is pinned by the grain boundary. In this model the shear stress at grain boundary (τ_{gb}) is given by

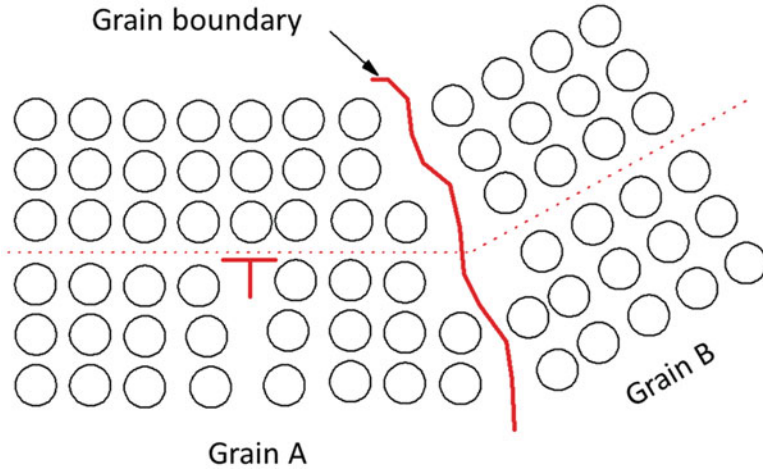


Fig. 1.7 Dislocation-grain boundary interaction

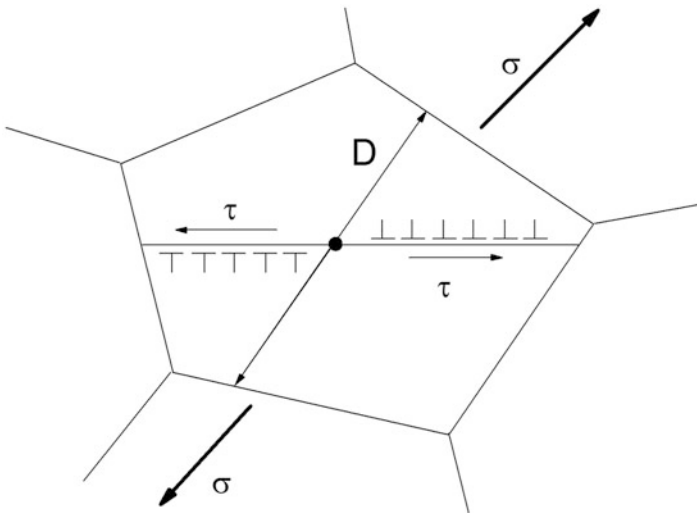


Fig. 1.8 Stress leading to dislocation sliding inside the grain

$$\tau_{bg} = \tau_{eff} \sqrt{\frac{D}{4r}} = \tau_a - \tau_0 \sqrt{\frac{D}{4r}}$$

where r is the distance from the point of dislocation generation and the grain boundary. Finally, the shear stress necessary for the dislocation movement taking into account the crystal interior and the grain boundary resistances is given by

$$\tau_a = \tau_0 + \tau_{bg} \sqrt{\frac{4r}{D}}$$

that is the Hall-Petch relationship in terms of shear.

Some researchers observed that the capacity of generating dislocations inside the grain is related to the parameter

$$\mu = \frac{\text{emitted dislocation length}}{\text{grain area}}$$

that is related to the dislocation density (ρ) by

$$\rho = \frac{3\mu}{D}$$

Finally, the Hall-Petch relationship can be expressed by

$$\tau = \tau_0 + \alpha Gb \sqrt{\frac{3\mu}{D}} = \tau_0 + k'_y D^{-1/2}$$

where α is a parameter depending on the crystal structure, G is the shear modulus, and b is the Burgers vector.

Now, the most common dislocation generation mechanism in the grain interior is given by the Frank-Read source. By reducing the grain size the dislocation loop dimension is reduced up to disappearance for nanosized grains (Fig. 1.9).

So, by decreasing the grain size, the material strength increases because of the limited dislocation generation and the limited space for sliding before the interaction with the grain boundary (Fig. 1.10).

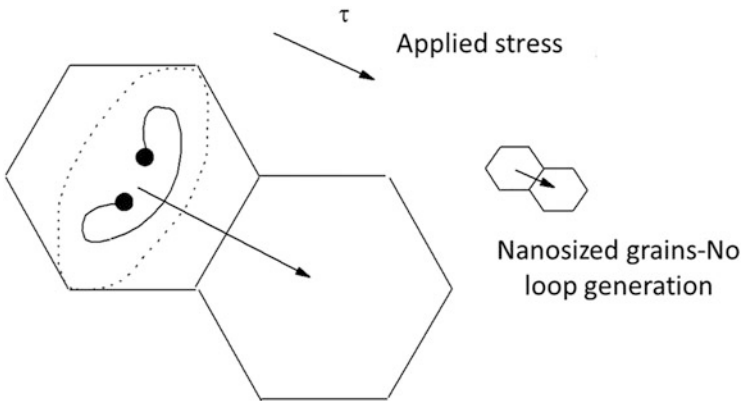


Fig. 1.9 Dislocation generation inside the grains

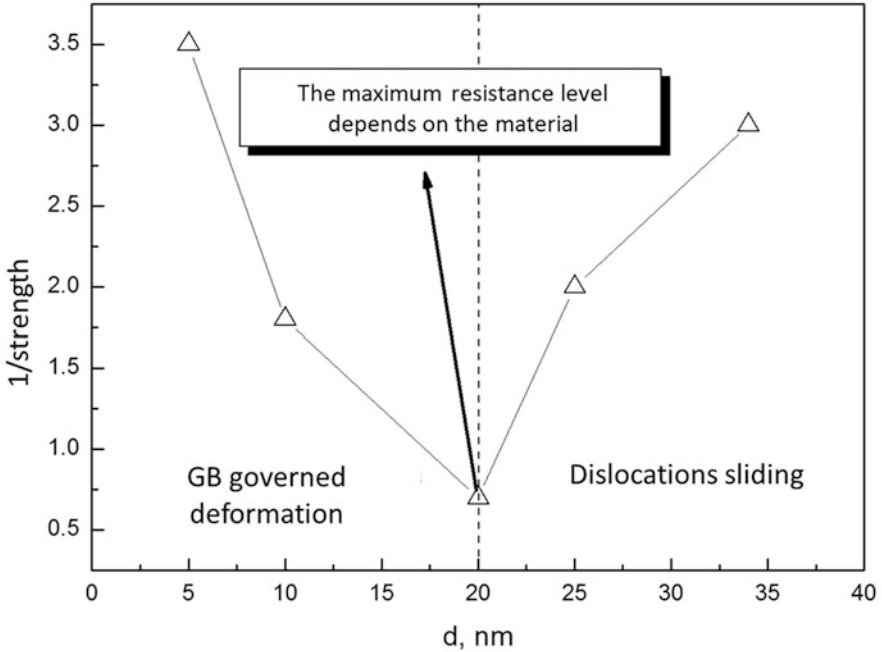


Fig. 1.10 Strength variation vs. grain size in pure Cu

Dislocation activity is grain size dependent. Full dislocation activity may be inhibited at very small grain sizes as partial dislocation activity becomes more favorable. In terms of the Orowan relation, the resolved shear stress required for expansion of a dislocation loop with a diameter of D is

$$\tau_{\text{RSS}} = \frac{\mu b}{D}$$

where μ is the shear modulus and b is the Burgers vector of dislocation. Full dislocation multiplication requires that Frank-Read-type sources have a minimum grain size (D^*) at the yield strength (σ_y) of

$$D^* = \frac{\mu b}{\frac{\sigma_y}{m}}$$

where $1/m$ is the average Schmid factor for polycrystals ($m = 3$). This would mean that as grain size becomes smaller than D^* full dislocation is inhibited and partial dislocation activity becomes dominant in the deformation of most grains, hence enhancing the GB relaxation process (Zhang et al. 2018). As the GB relaxation process is triggered by plastic deformation, it may not happen in the nanograined

metals which possess high GB energy and hence poor thermal stability (Zhou et al. 2018; Wrobel 2012).

According to the results of kinetic modeling, carried out within the developed dislocation model, considering the wholeness of all the possible deformation mechanisms and presenting the development of the well-known composite models, the temperature alteration of the plastic deformation brings to the activation or suppression of some deformation processes in GBs of Cu with different microstructures. On the one hand, the temperature increases as well as the hydrostatic pressure growth activates the work of the Frank-Read sources. The efficiency of GBs as the sinks for dislocations increases. Both the annihilation of the screw dislocations during their double cross-slip and their annihilation during the nonconservative motion increase (Alexandrov and Chembarisova 2012).

In the intermediate nanocrystalline grain size range above approximately 10 nm and below 100 nm, it is likely that there exists competition between conventional lattice dislocation slip and diffusional deformation, with the relative contributions of these deformation modes being dependent upon the distribution of grain sizes (Gapontsev and Kondrat'ev 2002).

If the deformation is governed by the dislocation sliding, the strength increases as the grain size decreases. This continues up to a grain size limit, then the deformation is governed by the grain boundary deformation, and the strength starts to decrease as the grain size decreases; this is commonly known as the Hall-Petch inversion (Fig. 1.11).

The Hall-Petch inversion has been observed for many nanocrystalline metals produced via different routes (Bober et al. 2016). The shear deformation process of

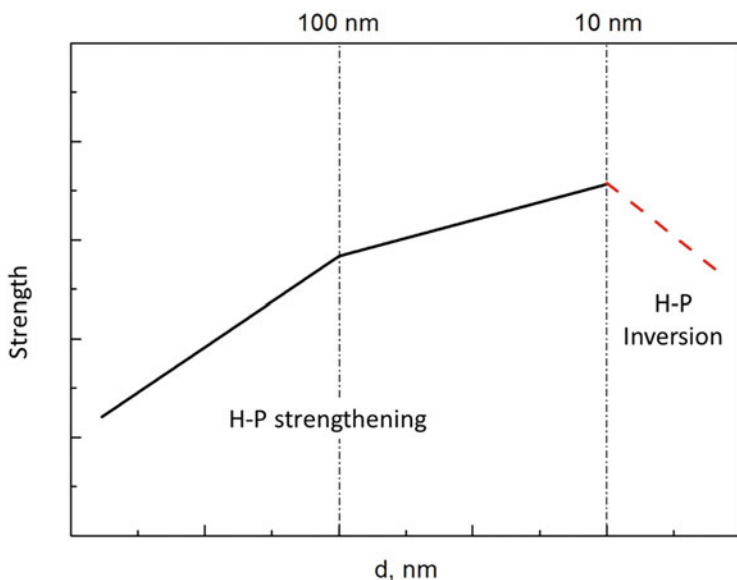


Fig. 1.11 Qualitative crystal strength vs. grain size

nanocrystals based on assuming an athermal deformation has been modeled. In accordance with them the shear propagation is composed of the grain boundary sliding and the shear deformation of crystalline matrix occurring mostly near the grain boundary plane. The latter deformation may be a twinning deformation, partial dislocation glide, or a stress-induced amorphization leading to a grain boundary thickening (Sitek and Degmová 2006). Because of the distribution of the angles between the boundary planes and the shear plane its width varies from a boundary to another. If the thickness of the boundary is t , the average width of the boundary region in the shear plane is αt , where α is about 2. If the stress necessary to propagate the shear front in the boundary region is σ_b and that in the crystalline matrix is σ_c , then $\sigma_c > \sigma_b$, and hence as the grain boundary region increases the deformation stress decreases, leading to an inverse H-P relation. Along the shear front, the fraction of the boundary region is $\alpha t/d$ and that of the crystalline region is $1 - \alpha t/d$. Thus, the stress necessary to propagate the shear front is written as

$$\sigma = \left(1 - \frac{\alpha t}{d}\right)\sigma_c + \left(\frac{\alpha t}{d}\right)\sigma_b$$

The value of σ_c is material dependent while the value σ_b depends on the material, its purity, the processing to produce the nanocrystal, and the history of the treatment, because the structure of the boundary which affects σ_b should be sensitive to the purity and processing.

The quantitative variation of yield strength as a function of grain size for pure Ni, Cu, Fe, and Ti is shown in Fig. 1.12.

In Zhao et al. (2003) it is shown how the melting temperature of the nanostructured crystals decreases with decreasing particle size; the Hall-Petch relationship becomes limited and is no longer sufficient for grain sizes less than around 15–30 nm. They proposed a model where there is a numerical maximum whose location depends on the bulk melting enthalpy of the crystals:

$$\sigma(d) = \sigma_0 + \left[k_t + k_d D^{-\frac{1}{2}}\right] \exp\left[-\frac{1}{T_d} \frac{H_m/3R}{\frac{D}{6h} - 1}\right]$$

where

$$k_t = k'_t \exp\left[\frac{T_{m0}}{2T_d}\right]$$

$$k_d = k''_d \exp\left[\frac{T_{m0}}{2T_d}\right]$$

$$H_m = T_{m0}S_m$$

If the bulk melting enthalpy is applied to nanostructured Ni (Fig. 1.13), the transition grain size can be calculated.

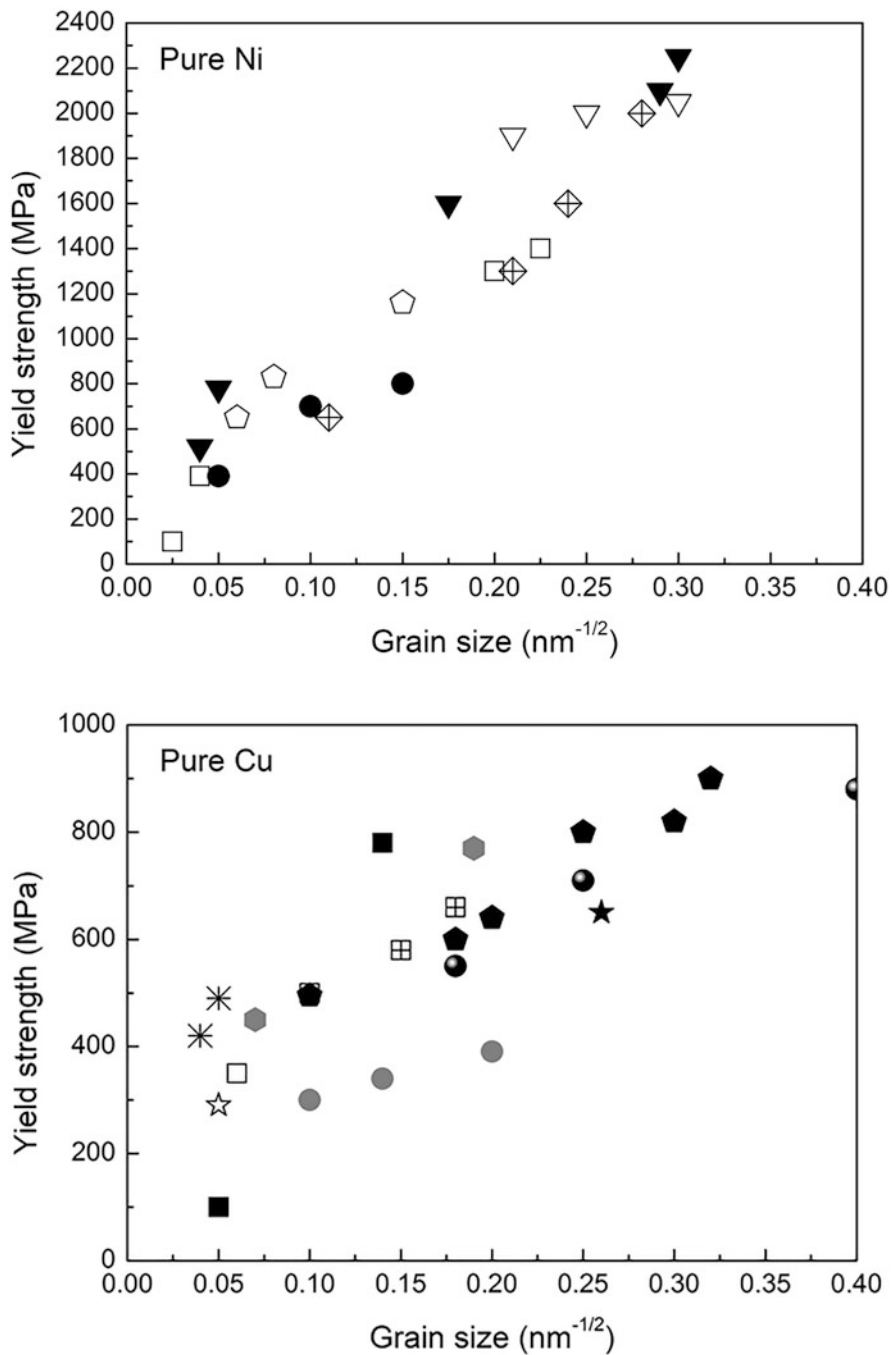


Fig. 1.12 Yield strength vs. grain size for pure Ni, Cu, Fe, and Ti

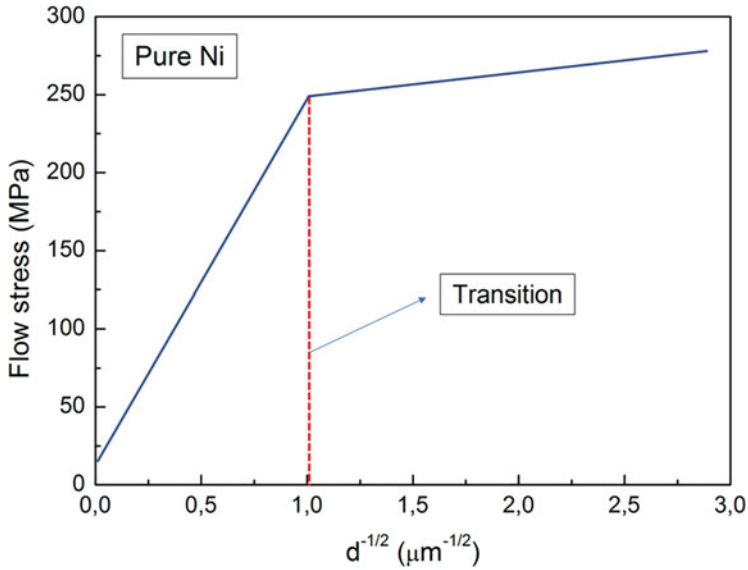


Fig. 1.13 Flow stress vs. grain size based on the bulk melting enthalpy

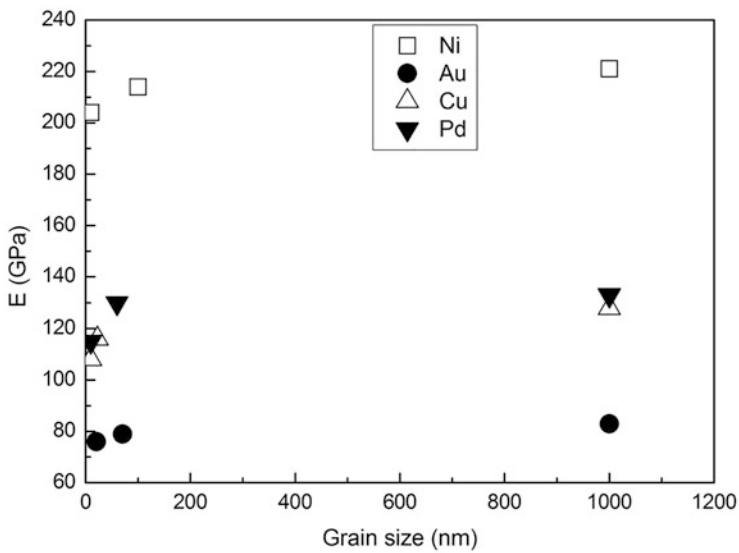


Fig. 1.14 Young's modulus variation with grain size

Another physical property to vary as the grain size is reduced is the Young's modulus. In Fig. 1.14 the E variation with grain size for different electrodeposited pure metals is shown.

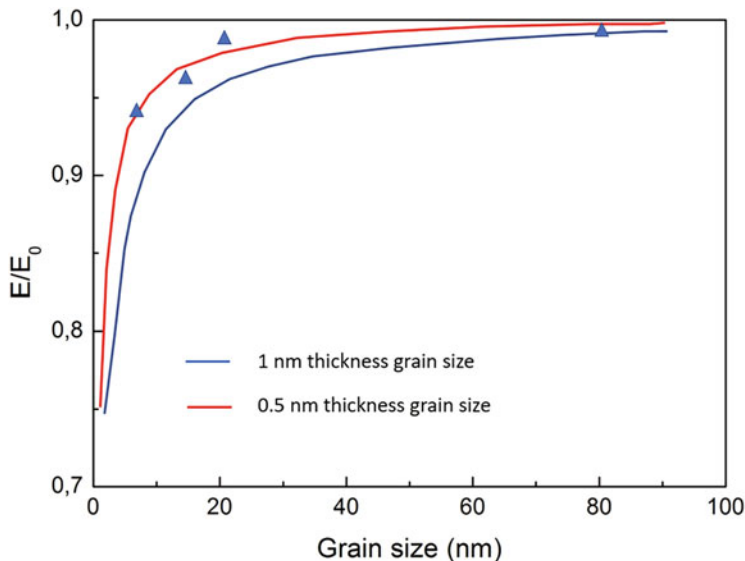


Fig. 1.15 Young's modulus variation with grain size for nanocrystalline Fe

Given that the values of a material's elastic constants reflect the bonding nature of its constituent atoms, it seems logical to expect that nanocrystalline materials would exhibit different moduli of elasticity compared to coarse-grained polycrystalline solids because of the high volume fraction of atoms located at or near the grain boundaries, triple junctions, and quadruple nodes (Ramesh 2009). In particular, since the degree of atomic structural disorder is greater within a grain boundary as compared to the crystal lattice, the average atomic distance within it is generally known to be larger. It could then be concluded that the grain boundary as a whole exhibits a lower bond strength and, therefore, has local elastic moduli values lower than those of the lattice (Zhu and Zheng 2010).

Different calculations and experimental analyses of pure Fe revealed a remarkable difference in Young's modulus with grain size (Fig. 1.15).

It is known that ultrafine-grained materials follow the Hall-Petch grain size strengthening behavior into the nanocrystalline regime. On the other hand, at some grain size transition from the regular to inverse Hall-Petch has also been reported in literature. The dependency of yield strength or hardness on grain size may become weaker, and even reverse at extremely fine-grain sizes. This phenomenon is known as the "inverse Hall-Petch effect" or "softening effect" (Carlton and Ferreira 2007). The reasons for the transition are a changing balance between competing deformation mechanisms (Zhou and Qu 2019). When conventional grain size metals are deformed at room temperature strain is carried exclusively by dislocations. Under these circumstances, grain boundaries influence deformation but they are not carriers of it. At the nanoscale, grain boundaries can mediate deformation more directly by sliding and shear-coupled migration or serving as dislocation sources and sinks.

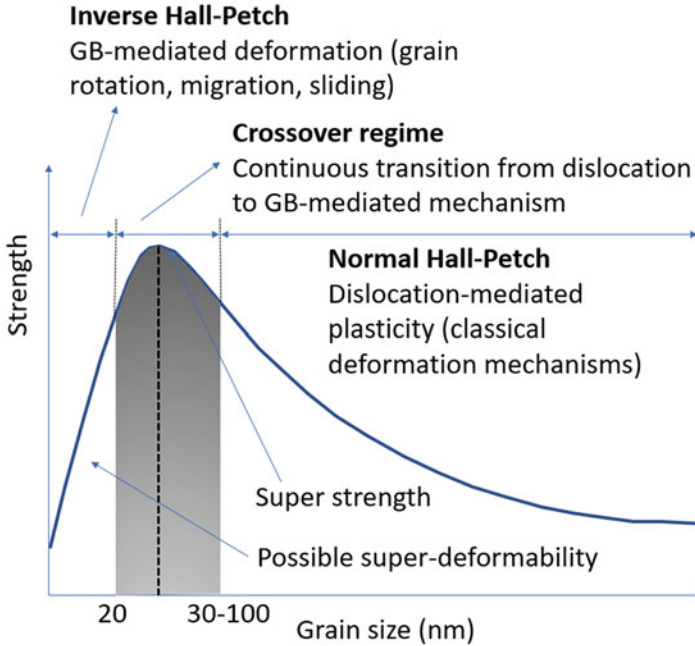


Fig. 1.16 Hall-Petch behavior at different length scales

There is strong evidence that applied shear stresses can drive rapid, diffusionless motion of nanocrystalline grain boundaries via shear coupling. Grain boundary sliding can also permit grains to slide past their neighbors, with accommodation provided by atomic shuffling. It has even been proposed that this leads to large grain rotations. At the same time, typical dislocation-based mechanisms become difficult to operate. From an atomistic point of view, there is a probability for atoms on a dislocation core to be absorbed by the grain boundary. The larger the grain size, the larger the number of atoms absorbed by the grain boundary, if the dislocation is also to be absorbed. Thus, for larger grain sizes, the probability for dislocation absorption by the grain boundary is lowered.

The most accepted general behavior is schematically shown in Fig. 1.16.

Below about 100 nm, there simply is not the space inside grains to activate conventional sources, or form pileups or dislocation tangles. This has the remarkable consequence that dislocation storage does not occur. Instead, dislocations are likely to be emitted from the boundaries, cross the grain, and be absorbed at the opposite side, without ever encountering another dislocation (Zhang et al. 2020).

The dislocation-based model (Yamakov et al. 2002) is based on the principle that dislocations are responsible for the flow in nanocrystalline materials and the dislocation energy is reduced as the grain size decreases. Anyway, by reaching a threshold grain size value twinning and partial dislocation generation lead to an increase in flow stress reducing the material strength (Zhu et al. 2008). Another